Metabolic and Cellular Alterations Underlying the Exaggerated Renal Prostaglandin and Thromboxane Synthesis in Ureter Obstruction in Rabbits

INFLAMMATORY RESPONSE INVOLVING FIBROBLASTS AND MONONUCLEAR CELLS

TADAO OKEGAWA, PHYLLIS E. JONAS, KATHERINE DESCHRYVER, AKIYOSHI KAWASAKI, and PHILIP NEEDLEMAN, *Departments of Pharmacology and Pathology, Washington University Medical School, St. Louis, Missouri 63110*

ABSTRACT Unilateral ureter obstruction in rabbits produced profound changes in endogenous and exogenous renal arachidonic acid metabolism. Isolated perfused hydronephrotic kidneys (removed after 3 or 10 d of ureter obstruction) responded to bradykinin stimulation with a markedly enhanced release of prostaglandin E_2 and thromboxane A_2. Reversal (3 or 10 d) of the ureter obstruction resulted in a reduction in the vasoactive peptide-induced release of prostaglandin E_2 and thromboxane A_2 from the perfused hydronephrotic kidney. However, postobstruction reversal of prostaglandin production by the agonist-stimulated perfused kidney was not reflected in the cortical microsomal cyclooxygenase activity, which is greatly enhanced during ureter obstruction and does not decrease after removal of the obstruction. Histological analysis of the renal cortex in rabbits with ureteral obstruction revealed a proliferation of fibroblast-like cells and the presence of mononuclear cells; removal of the obstruction did not result in a disappearance of cortical fibroblasts but did result in a decrease of monocytes. The critical involvement of mononuclear cells in the exaggerated arachidonate metabolism that occurs during hydronephrosis was exhibited by the demonstration that: (*a*) only the perfused hydronephrotic rabbit kidney responded to administration of endotoxin with a sustained release of prostaglandin E_2 and thromboxane A_2; (*b*) the contralateral rabbit kidney, which is devoid of mononuclear cells, did not respond to endotoxin; and (*c*) the hydronephrotic cat kidney, which exhibits a fibroblast proliferation with a low number of mononuclear cells, did not respond to endotoxin. Thus, proliferation of fibroblast-like cells and the presence of mononuclear cells appear to be involved in the exaggerated prostaglandin and thromboxane production underlying hydronephrosis. The increase in microsomal cyclooxygenase activity is apparently most closely correlated with the increased fibroblastic activation and cellularity, whereas mononuclear cells (possibly via monokines) seem to be critical for the markedly enhanced prostaglandin and thromboxane release induced by endotoxin and bradykinin.

INTRODUCTION

Perfused normal rabbit kidney releases modest amounts of prostaglandin (PG)[1] E_2 in response to vasoactive peptides (bradykinin and angiotensin II) (1). In microsomes prepared from the normal kidney, the medulla is the primary site of arachidonic acid metabolism; much less PG production occurs in the cortex

Preliminary data was presented at the Federation of American Societies for Experimental Biology meeting in New Orleans, April 1982.

Dr. Okegawa's and Dr. Kawasaki's permanent address is The Ono Research Institute, Osaka, Japan. Address all correspondence to Dr. Needleman.

Received for publication 18 May 1982 and in revised form 22 September 1982.

[1] *Abbreviations used in this paper*: CLK, contralateral (unobstructed) kidney; HHT, 12-hydroxy-heptadecatrienoic acid; HNK, hydronephrotic kidney; PG, prostaglandin; TxA_2 and TxB_2, thromboxane A_2 and B_2, respectively.

(2). Unilateral ureter obstruction (hydronephrosis) for several days results in a marked facilitation of: (*a*) PGE_2 release from an isolated perfused kidney (3); (*b*) cortical microsomal arachidonate metabolism (4, 5); and (*c*) cortical slice PG release (6). In addition, the perfused hydronephrotic kidney (HNK) has been demonstrated to release thromboxane A_2 (TxA_2). The thromboxane synthetase activity is clearly evident in HNK cortical microsomes, whereas this enzyme is not detectable in normal or contralateral unobstructed rabbit kidneys (CLK) (4, 7). Other models of renal damage in rabbits, such as renal venous constriction (8) and glycerol-induced renal failure (9), are also associated with an unmasking of renal thromboxane biosynthesis. Thus, there are quantitative and qualitative changes occurring simultaneously in renal arachidonate metabolism associated with renal damage. The renal thromboxane production resulting from ureter obstruction has been associated with renal vasoconstriction and the reduced glomerular filtration rate that also occurs with hydronephrosis (10). We have been able to demonstrate that the thromboxane synthesis stimulated by bradykinin and angiotensin in the perfused HNK results in a pronounced renal vasoconstriction that can be reversed by a thromboxane synthetase inhibitor (11).

The mechanism and cell types that underlie this unmasking of renal cortical arachidonate metabolism attendant to ureter obstruction are the focus of this study. Nagle et al. (12, 13) have demonstrated that ureter obstruction in rabbits is associated with an enlargement of the renal cortical interstitial space with a distinct proliferation of a fibroblast-like cell and an infiltration of mononuclear cells. Our strategy was to evaluate the relationship of the appearance of these cell types in the HNK relative to endogenous and exogenous renal arachidonic acid metabolism. Our opportunity to study this problem was enhanced by the development of the experimental capability of relieving the ureter obstruction and reversing the stimulus that underlies this renal pathophysiological model.

METHODS

Materials. [^{14}C]arachidonic acid (55 Ci/mol), [^{3}H]PGE_2, and [^{3}H]thromboxane B_2 (TxB_2) (100 Ci/mmol) were purchased from New England Nuclear (Boston, MA). Prostaglandin standards were kindly supplied by Dr. John Pike of the Upjohn Company (Kalamazoo, MI). Indomethacin was the gift of Merck, Sharp & Dohme (West Point, PA). The unlabeled arachidonic acid was purchased from Nu-Chek Prep. Inc. (Elysian, MN) and the endotoxin (lyophilized *Escherichia coli*; 055:B5) from Difco Laboratories (Detroit, MI).

Ureter obstruction, release of obstruction, and kidney perfusion. Unilateral ureteral obstruction was carried out in male New Zealand white rabbits (2–3 kg) by a previously described procedure (3). Briefly, complete ureter obstruction of the left kidney was performed in a pentobarbital (30 mg/kg) anesthetized rabbit through a small abdominal incision by tying a silk suture around the ureter near the bladder.

Animals that were to have the ureter obstruction released were anesthetized either 3 or 10 d after the original ureter ligation. The abdominal incision was reopened and a polyethylene cannula (PE-160, Clay-Adams, Div. of Becton, Dickinson & Co., Parsippany, NJ; 1.14 mm i.d.) was inserted into the urine-engorged ureter above the ligation. The cannula was passed subcutaneously along the back and exteriorized at the head. The initial cannulation was associated with a copious urine flow with some blood being present for ~1 h. The ureter cannula was examined daily and usually remained patent for the desired recovery period (3 or 10 d).

On the morning of the perfusion experiment, the animals were anesthetized with pentobarbital (30 mg/kg, i.v.), heparin (250 U/kg i.v.) was administered, and their renal arteries were cannulated. The kidneys were excised, placed in a warming jacket, and perfused at 10 ml/min with oxygenated (O_2:CO_2–95:5%) Krebs-Henseleit media at 37°C. The venous effluent from the HNK and CLK was allowed to flow directly over smooth muscle assay organs: rabbit thoracic aorta, to indicate the presence of TxA_2-like activity; and chick rectum and rat fundal stomach, to indicate the presence of PGE_2-like activity. Indomethacin (1 μg/ml) was perfused directly over the assay tissues to eliminate the possibility that the assay tissues might release endogenous PG (14).

Arterial administration of a bolus injection of bradykinin stimulates a transient (3–5 min) release of arachidonate metabolites from the perfused kidney. Thus, 50 ml (i.e., 5 min at 10 ml/min) of pre- and post-stimulus effluent was collected when the agonist employed was bradykinin. On the other hand, we discovered that a bolus injection of endotoxin (100 ng) produces slowly initiated but chronic release of arachidonate metabolites from the HNK. So, in the case of the endotoxin experiments, a pre-stimulus 50-ml portion of renal venous effluent was collected. After administration of the endotoxin, a 50-ml aliquot was collected every 30 min for 3 h. The 50-ml effluents were very well-mixed and a 500-μl aliquot was saved and frozen (−20°C) for subsequent radioimmunoassay (RIA).

The isolated rabbit kidneys were frozen upon completion of the perfusion experiments and were stored at −70°C.

Preparation of microsomes. The frozen (−70°C) kidney was thawed and was separated into cortex and medulla. Tissues were diced and homogenized (Tekmar homogenizer [Tekmar Co., Cincinnati, OH]) in four volumes (wt/vol) of 100 mM phosphate buffer, pH 7.8, containing 1% bovine serum albumin (BSA) and 10 mM EGTA. The albumin was included in order to trap any fatty acid release during the homogenization, and the EGTA was present to prevent the activation of tissue phospholipase by Ca^{++}. Cyclooxygenase activity is vulnerable to autodestruction in the presence of arachidonic acid (15) and we previously found that the presence of albumin and EGTA during the tissue preparation markedly enhanced the arachidonic acid metabolism (16). The homogenate obtained was centrifuged at 8,000 *g* for 15 min in a refrigerated Sorvall centrifuge (E. I. Du Pont de Nemours & Co., Inc./Sorvall Instruments Div., Newton, CT). The supernatant was further centrifuged at 100,000 *g* for 60 min in a Beckman L2-75B ultracentrifuge (Beckman Spinco, Palo Alto, CA). The surface microsomal pellet was washed

twice with 100 mM phosphate buffer to remove the albumin. The microsomal pellet was resuspended in phosphate buffer in a volume equal to one-quarter of the original wet weight of the tissue. The protein concentration of the microsomal preparation was determined with fluorescamine by using BSA as the standard.

Kinetic analysis of the microsomal conversion of arachidonic acid. The reactions were carried out in phosphate buffer (0.1 M, pH 7.8) in a final volume of 150 μl in a siliconized 10 × 75-mm tube that contained 100–300 μg protein and 1 mM epinephrine. The tube was preincubated on a stirrer at 37°C for 1 min and the reaction was started by the addition of the arachidonic acid. For the kinetic studies, the fatty acid was varied from 0 to 160 μM. All reactions were run in duplicate. Because the reaction was linear for 10 min under these incubation conditions, all subsequent kinetic experiments were performed for 4 min at 37°C. The reaction was stopped with 1.4 ml of ice-cold RIA buffer (50 mM potassium phosphate buffer, pH 7.4, containing 0.1% BSA). After rapid mixing, a 20-μl aliquot was added to 180 μl of RIA buffer, thus achieving the ~100-fold dilution necessary for the immunoassay of PGE_2.

Radiochemical experiments. Cortical or medullary microsomes were incubated with [^{14}C]arachidonate (300,000 cpm, 1 μg) in the presence of 1 mM epinephrine for 30 min at 37°C. Reactions were stopped by the addition of 2 N formic acid to bring the reaction mixture to pH 3.5. The mixture was extracted twice with two volumes of ethyl acetate. The extracted lipids were concentrated and chromatographed with unlabeled PG standards on silica gel G thin-layer plates (Brinkmann Instruments Inc., Westbury, NY) in a solvent system of chloroform:methanol:acetic acid:water (60:30:3:0.1). PG standards were visualized by using iodine vapor and the plates were analyzed in a Vangard radioisotope scanner (Packard Instrument Co., Inc., Downers Grove, IL). The resolved thin-layer plates then underwent autoradiography by exposure to x-ray film (Kodak XAR-5, Eastman Kodak Co., Rochester, NY).

RIA. PGE_2 and TxB_2 were immunoassayed with rabbit antisera as previously described (17). The crossreactivities at 50% displacement of other PG with the antisera were as follows: (*a*) PGE_2 antiserum—6-keto-$PGF_{1\alpha}$, 0.39%; $PGF_{2\alpha}$, 0.04%; TxB_2, 0.003%; and (*b*) for the TxB_2 antiserum—6-keto-$PGF_{1\alpha}$, 0.009%; PGE_2, 0.012%; and $PGF_{2\alpha}$, 0.025%. The media from the microsomal incubations, as well as the renal venous effluent collected from the isolated perfused kidneys, did not alter the immunoassay standard curve for either the PGE_2 or the TxB_2.

Histological techniques. The normal, hydronephrotic, postobstructed and contralateral kidneys were rapidly excised and bivalved (n = 4–5 for each category). Small fragments of renal cortex were rapidly fixed in 2.5% glutaraldehyde in phosphate buffer, and processed for electron microscopy. The specimens were postfixed in 1% osmium, dehydrated in a series of alcohols, and embedded in Spurr.

1-μm sections stained with toluidine blue were examined and, in areas where glomeruli were present, further thin sectioning was performed. The relative interstitial cellularity was evaluated on these thin sections in five samples from different areas of the cortex in each experiment, at ×400.

Uranyl acetate- and lead citrate-stained thin sections on copper grids were viewed in a Philips 300 electron microscope (Philips Electronic, Mahwah, NJ). The nature of the mononuclear cell involved was then further determined and relative cell populations counted. A mean of 18 different interstitial spaces was evaluated (range 9 to 25) for each experimental category. All morphologic observations were made on coded specimens, without knowledge of the biochemical data or experimental category.

RESULTS

PGE_2 and TxA_2 release from perfused hydronephrotic and postobstructed kidneys. Isolated perfused rabbit kidneys were challenged each hour with a bolus injection of a fixed high dose (500 ng) of bradykinin. The renal venous effluent was collected for RIA before and after stimulation. A normal or unobstructed perfused rabbit kidney released 100–200 ng of PGE_2/50 ml renal perfusate (i.e., 5-min collection of perfusate at a flow rate of 10 ml/min includes >90% of the PGE_2 released by the agonist) in response to administration of 500 ng of bradykinin. Rabbit kidneys obstructed in vivo for 3 or 10 d before perfusion released comparable amounts of PGE_2 (both the 3- and 10-d HNK released ~5,000 ng/50 ml effluent after 8 h of perfusion) in the renal venous effluent after bradykinin stimulation (Fig. 1).

When compared with the CLK (3.5–3.8 cm long), the HNK was considerably enlarged after 3 or 10 d of obstruction (4.5–5.0 cm long), had a rigid texture, and occasional hemorrhages were present on the surface. When ureter obstruction was relieved by cannulation above the ligature (and urine allowed to flow freely in vivo for 3 to 10 d before the perfusion experiment), the kidneys were reduced in size (compared with the HNK) and resembled the CLK. There was a 50 and 90% reduction of bradykinin-induced PGE_2 release after 3 or 10 d of in vivo postobstruction, respectively (Fig. 1). The reversibility of the peptide-induced PGE_2

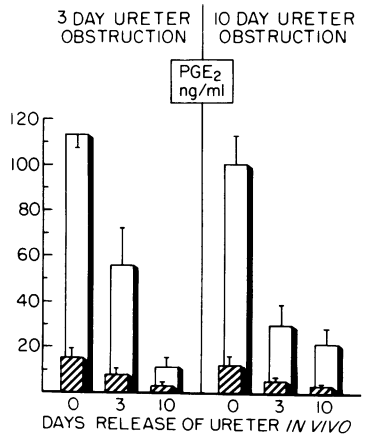

FIGURE 1 Bradykinin-induced release of PGE_2 from perfused hydronephrotic and postobstructed rabbit kidneys. The data shown were obtained by comparing basal (hatched bars) and bradykinin-induced (500 ng bolus, open bars) PGE_2 release after 8 h of perfusion, and represent the mean±SE for four kidneys per group.

release was just as readily achieved when the initial obstruction was for 10 d as for 3 d.

A normal or contralateral unobstructed kidney does not synthesize or release detectable amounts of TxB_2. Bradykinin injection resulted in the release of 250 ng/50 ml renal venous effluent of TxB_2 from isolated perfused kidney obtained after 3 d of ureter ligation; 10 d obstruction resulted in a further enhancement of TxB_2 release (600 ng/50 ml) (Fig. 2). Intrarenal infusion of the thromboxane synthetase inhibitor, OKY-1581 (1.5 μg/ml), eliminated the appearance of TxB_2 in the renal venous effluent (11). Postobstructive reversal of the hydronephrosis resulted in a pronounced reduction in the bradykinin-induced thromboxane release (Fig. 2).

Arachidonic acid metabolism by hydronephrotic and postobstructed kidney microsomes. A comparison of the kinetics of the cyclooxygenase activity present in the various kidneys was performed under conditions of linearity by using varying amounts of arachidonic acid as substrate. The maximum velocity (V_{max}) for the enzymatic conversion of arachidonate to PGE_2 in the normal kidney or CLK cortex was 36 pmol PGE_2 formed/mg microsomal protein per min at 37°C and 276 pmol/mg per min for the medulla. 3 d of ureter obstruction resulted in a marked increase in cortical cyclooxygenase activity (145 pmol/mg per min) compared with unobstructed controls; however, HNK medullary production of PGE_2 was still about four times higher than the HNK cortical microsomes (Table I). The V_{max} for the conversion of arachidonic acid into TxB_2 was 10 pmol/mg per min in the control cortex and had risen to 66 and 373 pmol/mg per min after 3 or 10 d of ureter obstruction, respectively.

TABLE I
Rate of Rabbit Renal Microsomal Arachidonic Acid Conversion to PGE_2

	PGE_2 formation		
	K_m	V_{max}	
	μM	pmol/mg/min	n
3-d HNK cortex			
0-d release	13	145	3
3-d release	19	136	4
10-d release	18	209	3
3-d HNK medulla			
0-d release	12	552	3
3-d release	12	533	4
10-d release	13	563	3
10-d HNK cortex			
0-d release	21	341	4
10-d release	15	192	4

The values are the means and n indicates the number of kidneys studied in each group. The SEM for the Michaelis constant (K_m) values (from Lineweaver-Burk plots) was 5–15%, and for the maximum velocity (V_{max}), 10–25%.

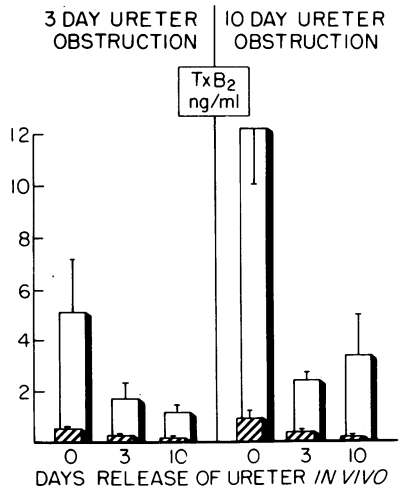

FIGURE 2 Bradykinin-induced release of thromboxane (TxB_2) from the perfused hydronephrotic and postobstructed rabbit kidney. The TxB_2 was measured from the same aliquots collected for the PGE_2 assays shown in Fig. 1.

In sharp contrast to the reversal of the peptide-induced arachidonic acid metabolism by the perfused kidney (Figs. 1 and 2), the cortical and medullary microsomal metabolism of arachidonic acid by the HNK was not reversed by the release of the ureter obstruction (Table I). Comparable data were obtained when the microsomal conversion of arachidonate to TxB_2 was analyzed (not shown). The kinetic reactions of either PGE_2 or TxB_2 were measured by RIA; thus, an alteration of the pattern of arachidonate metabolites might go undetected. In view of the surprising separation of endogenous (bradykinin-induced in the perfused kidney) and exogenous microsomal arachidonate metabolism, we analyzed the product profile of [^{14}C]arachidonate conversion by renal microsomes. Consistent with the kinetic data, there was no difference in the relative qualitative or quantitative conversion of the labeled fatty acid by cortical or medullary microsomes from either hydronephrotic or postobstructed kidneys (Fig. 3). The thin-layer plates were scraped and counted for an indication of the relative abundance of each product. For example, in the 10-d HNK cortex with 0-d release we found that the products of thromboxane synthetase [i.e., the sum of TxB_2 and 12-hydroxy-heptadecatrienoic acid (HHT)] accounted for 32% of the metabolized arachidonate, PGE_2 represented 13%, whereas PGD_2 and $PGF_{2\alpha}$ were

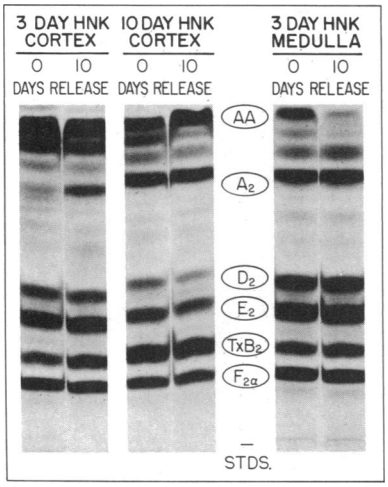

FIGURE 3 Autoradiogram of the thin-layer chromatographic separation of the arachidonate metabolites produced by cortical and medullary microsomes. The following abbreviations were employed: AA, arachidonic acid; A_2, PGA_2; D_2, PGD_2; E_2, PGE_2; $F_{2\alpha}$, $PGF_{2\alpha}$; and STDS-unlabeled PG, standards-position visualized with iodine vapors.

only 6 and 9%, respectively. These latter two eicosanoids do not influence renal resistance and probably reflect the nonenzymatic breakdown of the endoperoxide. The cyclooxygenase metabolites ($PGF_{2\alpha}$, TxA_2, PGE_2, PGD_2, and HHT) were eliminated by preincubating the microsomes with indomethacin (1 μg/ml), and the TxB_2 and HHT bands (which migrate just above the PGA_2 standard) were eliminated by the thromboxane synthetase inhibitor, OKY-1581 (not shown).

Histological studies. In normal or contralateral (unobstructed) kidneys, the outer cortical interstitial space, between tubules and vessels, is narrow and triangular under physiologic circumstances and contains the interstitial cell bodies and their processes (Fig. 4). An occasional bundle of collagen may also be present. There is no difference between the morphology of the normal control and the CLK. In the 3-d HNK, marked morphologic changes occurred in the cortical interstitium (Fig. 5). The interstitial space was considerably widened, and the cellular content was several cells thick. The increased cellularity is due to interstitial cells virtually surrounded by mononuclear cells, including monocytes and lymphocytes. Release of obstruction does not alter the number of interstitial fibroblasts but does result in a reduction in the number of monocytes (Fig. 6).

The relative cell populations present are summarized in Table II. In the postobstructive release experiments at 10 d, the overall cellularity was slightly decreased and the still widened interstitial space contained abundant collagen fibers. Interstitial cells were large and their ratio to monocytes and lymphocytes increased threefold (Table I). The normal cat cortical

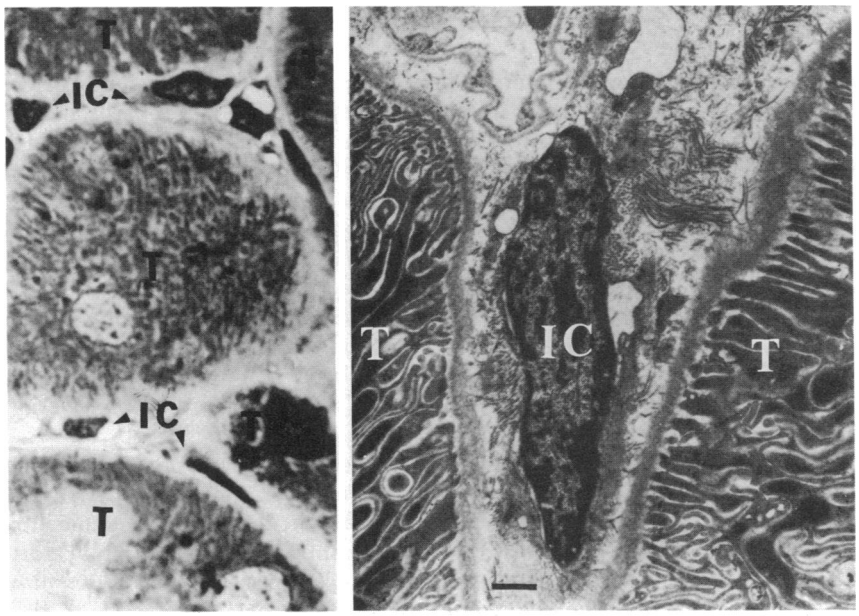

FIGURE 4 Light (left panel) and electron (right panel) micrographs of cortical interstitium from a normal kidney. Toluidine blue (×400), uranyl acetate, and lead citrate were used for tissue processing; the bar indicates 1 μm. The interstitial cell (IC) of the normal cortex is intimately related to the basement membrane of tubules (T).

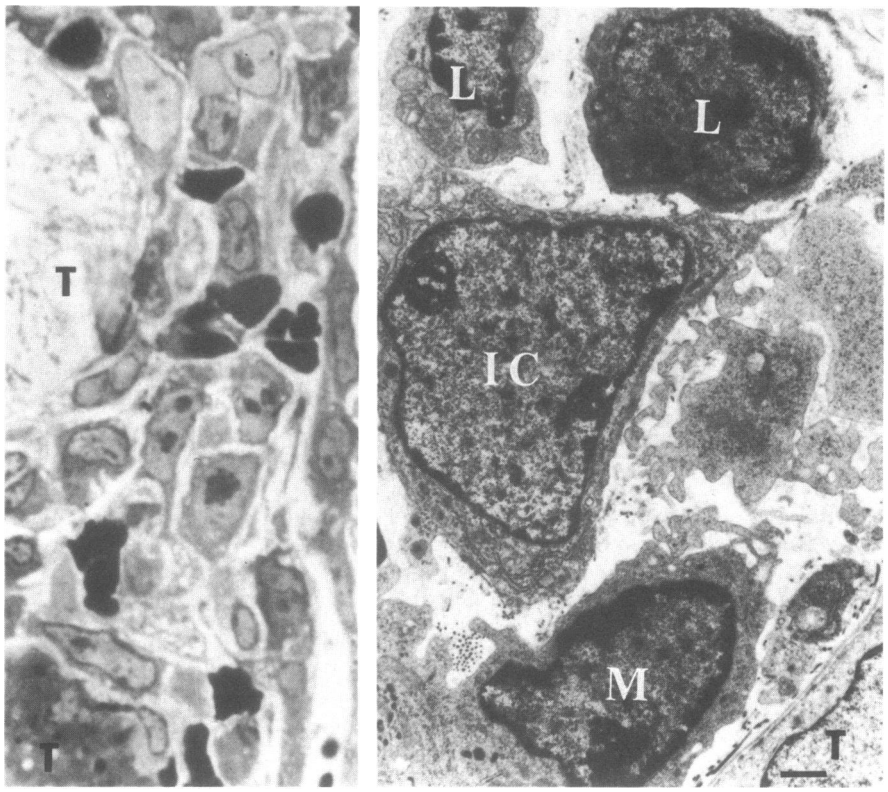

FIGURE 5 Light and electron micrographs of the cortex of the 3-d HNK. In the 3-d hydronephrotic cortical interstitium, the interstitial space is considerably widened. The interstitial cell is surrounded by a mononuclear infiltrate. T, tubules; IC, interstitial cell; L, lymphocyte; M, monocyte.

interstitium is small and is occupied by the interstitial cell. The interstitium is considerably enlarged in the 3-d hydronephrotic cat kidney, and the interstitial cell accounts for a large portion of the increased cellularity. The hydronephrotic cat kidney has considerably smaller monocytic infiltrate than the rabbit HNK. The ratio of fibroblasts:mononuclear cells in the cat HNK was 7:1, whereas in the rabbit HNK it was 1:1 (Table II).

At 10 d of hydronephrosis, the renal interstitium showed an increase in collagen bundles with a relative reduction of the cellular component, as compared to d 3. Interstitial cells constituted the major cell population, whereas lymphocytic cells represented the predominant mononuclear population. Fewer monocytes were present. Collapsed and reduplicated basement membrane was seen in the interstitial space, indicative of extensive tubular damage. 10 d postobstruction was characterized by further reduction in the cellular component of the interstitium, with increase in collagen fibers. The main cell present was the interstitial cell.

Endotoxin stimulation of arachidonate metabolism in perfused rabbit kidneys. The morphological evidence indicated the presence of cells that resembled macrophages and fibroblasts in the rabbit HNK, but not in the rabbit CLK or the cat HNK. In an attempt to evaluate the potential participation of the macrophage-like cells in the changes we measured during hydronephrosis, we studied the ability of endotoxin administration to stimulate prostaglandin production. Cultured macrophages have been previously demonstrated to release PGE_2 and TxB_2 in response to endotoxin (18–20). However, the lipopolysaccharide-stimulated macrophage metabolism of arachidonate was slow in onset and took several hours to manifest the response (19).

Ureter-obstructed and postobstructed kidneys were challenged on an hourly basis with bradykinin until the peptide elicited a pronounced TxA_2-like response (i.e., contraction of the rabbit aorta assay tissue) or PGE_2-like response (contraction of chick rectum assay strip). Endotoxin injection into the CLK resulted in the marginal appearance of detectable bioassayable or immunoassayable levels of PGE_2 (Table II) or TxB_2 in the renal venous effluent, whereas the HNK responded with a slowly developing but chronic contraction of

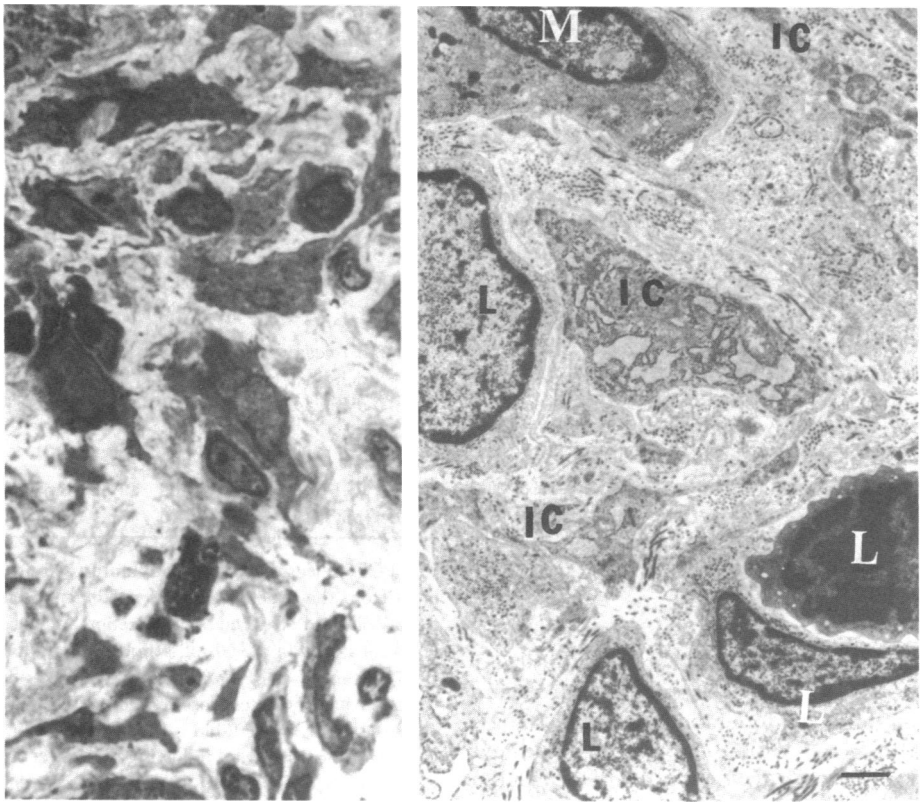

FIGURE 6 Light (left panel) and electron (right panel) micrographs of the cortex from the 3-d HNK after 10 d of postobstructive release. The still widened interstitial space is occupied by interstitial cells, lymphocytes, and few monocytes, and the amount of collagen is increased. Toluidine blue (×400), uranyl acetate, and lead citrate were used for tissue processing and the bar on the electron micrograph indicates 1 μm.

the vascular and nonvascular smooth muscle assay organs that lasted for hours. The RIA data were consistent with the bioassay data and indicated that the rabbit HNK, but not the CLK, possesses a cell type capable of releasing arachidonate metabolites in response to lipopolysaccharide (Table III). Relief of the ureter obstruction for 3 or 10 d, by insertion of the free-flowing cannula, caused a substantial decrease in endo-

TABLE II
Summary of Relative Renal Cortical Interstitial Cell Populations

Experimental group	Space	Total cells/ field (100%)	Renal cortical interstitial						
			Collagen	"Interstitial cell"		Monocyte		Lymphocyte	
				%	c/f	%	c/f	%	c/f
Rabbit									
Normal	Small	1.00	Scarce	100	1.00	0	0	0	0
CLK	Small	1.00	Scarce	100	1.00	0	0	0	0
3-HNK	3+	5.30	Scarce	45	2.43	37	1.70	18	0.95
3-HNK-10R	2+	4.50	Increased	58	2.61	17	0.76	25	1.12
Cat									
CLK	Small	1.00	Scarce	100	1.00	0	0	0	0
3-HNK	3+	4.57	Scarce	74	3.38	11	0.48	14	0.67

The assignment of the size of the interstitial space was compared relative to the normal renal cortex. The measurement of the number of cells/field (c/f) is described in Methods. The following abbreviations were employed: 3-HNK, 3-d hydronephrotic kidney; 3-HNK-10R, kidneys that were obstructed for 3 d followed by 10 d with the obstruction release; and c/f, cells per field.

toxin-induced PG release. Thus, both bradykinin or endotoxin stimulation of intrinsic arachidonic acid metabolism by the postobstructed kidney was markedly reduced, whereas the microsomal arachidonic acid conversion was still markedly facilitated (Table III).

We previously observed that the perfused cat HNK was only slightly more responsive in releasing PGE_2 in response to bradykinin or angiotensin II stimulation than was the cat CLK (17). Furthermore, the cat HNK did not release TxA_2 in response to agonist stimulation. Ureter obstruction in the cat resulted in a widening of the cortical interstitial space and a proliferation of fibroblasts, but very much fewer mononuclear cells were present than were observed in the rabbit HNK (Table II). Consistent with the sparse macrophage population, ureter obstruction of the cat kidney did not enhance the PGE_2 release induced by endotoxin (Table III).

TABLE III
Endotoxin- and Bradykinin-induced PGE_2 Release from Isolated Perfused Rabbit Kidneys

	Total PGE_2 release		
	Basal	Bradykinin (per 50 ml)	Endotoxin (per 3 h)
		ng	
Rabbit			
CLK (5)	89±13	177±48	892±800
3-day HNK:			
0-d release (5)	109±32	5,667±687	11,913±1,968
3-d release (4)	30±5	2,843±828	982±486
10-d release (4)	31±11	552±24	1,428±778
Cat			
CLK (3)	22±9	23±4	1,110±447
3-d HNK (3)	36±6	63±15	2,050±1,176

The PGE_2 released by the bradykinin (500 ng) injection is calculated from the concentration of product present in the 50-ml effluent collected after the bolus injection and corrected for the basal levels measured in the 50-ml sample collected before injection. The PGE_2 release by bradykinin is complete by 5 min postinjection. On the other hand, the response to endotoxin develops slowly and the value reported in the table is the concentration of PGE_2 accumulated over the 3-h period following the single bolus injection of 100 ng of endotoxin corrected for basal release. The bradykinin and endotoxin stimulations of the various perfused kidneys were performed at 6 and 6.5 h after initiation of perfusion, respectively. The values are the means±SE and the number in parentheses indicates the number of kidneys studied.

DISCUSSION

Complete, unilateral ureter obstruction (hydronephrosis) of the rabbit kidney results in profound changes in arachidonic acid metabolism and histologic changes in the involved kidney. In perfused kidneys isolated from rabbits with ureter obstruction (3 d), a marked enhancement of basal and vasoactive peptide (bradykinin and angiotensin II)-stimulated release of PGE_2 was observed (3). Further studies indicated that the perfused rabbit HNK released TxA_2 in response to peptide stimulation, and that the HNK, but not the CLK, possessed thromboxane synthetase activity (4, 7). Regional localization studies demonstrated that the enhanced PG biosynthesis occurred primarily in the cortex of the HNK (5, 6, 21).

Nagle et al. (12, 13) found that complete unilateral ureteral obstruction in the rabbit produced a diffuse fibrosis and parenchymal atrophy. 24 h after obstruction there were marked histologic changes in the rabbit cortex that became exaggerated with time. There was a pronounced widening of the interstitial space, an increase of fibroblasts, and the presence of mononuclear cells. The initial proliferative stimulus may be the increase in intrarenal pressure, which causes an enlargement of the interstitial space and decreases the contact of the few normally present fibroblasts with their environment, resulting in the promotion of fibroblast proliferation. Contact inhibition of fibroblast proliferation has been previously demonstrated (22).

The demonstration of mononuclear cells in close contact with the cytoplasmic processes of the cortical fibroblasts (13) may have profound implications in the progression of the histologic and metabolic changes involved in the renal injury. Leibovich and Ross (23, 24) found that abolition of circulating blood monocytes by the use of antimacrophage serum and steroids substantially delayed the appearance of fibroblasts at sites of tissue injury and suppressed the fibroblast proliferation rate. The macrophages also appear to actively modulate fibroblast PG biosynthesis. Several investigators have reported that conditioned media obtained from adherent mononuclear cell cultures contain a factor that is mitogenic for fibroblasts (23, 24) and in several instances it has been correlated to a marked (50–200-fold) stimulation of PGE_2 biosynthesis by dermal fibroblasts (25), by gingival fibroblast-like cells (26), and by synovial cells (27). Of course, the presence of a substantial number of macrophages in the damaged tissue introduces the possibility that these mononuclear cells themselves contribute to the arachidonic acid metabolites released by the HNK. Macrophages have a high arachidonic acid metabolic potential and have been demonstrated to synthesize PGE_2, TxA_2, PGI_2, and a number of lipoxygenase products (28, 29). To investigate the macrophage contributions to the HNK, we took advantage of the demonstration that

endotoxin stimulates cultured peritoneal macrophages to synthesize PGE_2 and TxA_2 (18, 28). We found that the perfused rabbit HNK, but not the rabbit CLK, responded to a bolus injection of endotoxin with a slowly initiated but sustained release of PGE_2 and TxB_2 (Table III). The time course of the release of arachidonic metabolites, especially thromboxane, from the perfused kidney compared favorably with the time course for metabolite production from cultured macrophages in response to endotoxin (19). We could observe macrophages only in the HNK, not in the CLK or normal kidney (Fig. 4, Table II); thus, the endotoxin induction of intrinsic arachidonate metabolism only by the obstructed rabbit kidney suggests preferential stimulation of the macrophage cell type. In addition, endotoxin has not been shown to stimulate PG production by the cultured fibroblast. However, endotoxin stimulation of PGE_2 release may in part be due to the release of factors by the macrophage which in turn stimulates fibroblast PGE_2 production, as has been demonstrated for synovial fibroblast-like cells (30). Furthermore, we previously showed that unilateral ureter obstruction of the cat kidney only modestly increased peptide-induced PGE_2 release and no thromboxane production was demonstrable (17). Histologic examination of the cat HNK indicated only the modest presence of macrophages. Now we have found that endotoxin does not stimulate PGE_2 or TxA_2 release from the perfused ureter-obstructed cat kidney.

Fig. 7 presents a schematic model of a sequence of events that could encompass many of the observations obtained in studies of hydronephrosis in the rabbit. Ureter obstruction causes a mechanical disruption and/or an immunologic (e.g., via the entrapped urine) stimulus in the cortex that triggers a regional inflammatory response resulting in stimulation of the interstitial cell and the presence of mononuclear cells. The macrophages, which are in direct contact with the fibroblasts, are capable of releasing a factor that stimulates: (*a*) fibroblast proliferation, (*b*) cortical microsomal cyclooxygenase activity, and (*c*) PGE_2 release (i.e., intrinsic arachidonate metabolism). The enhanced thromboxane synthetase levels and the TxA_2 release may come from the macrophages directly or from the activated fibroblasts.

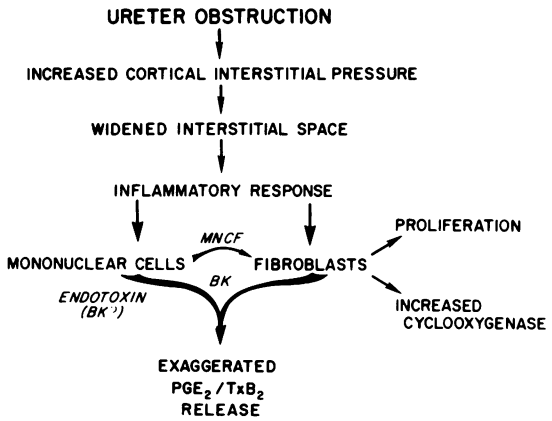

FIGURE 7 Hypothetical model of the cellular and metabolic alterations that occur attendant to ureter obstruction. MNCF is the abbreviation for the mononuclear cell factor that stimulates fibroblasts. BK, bradykinin.

The surprising feature of the postobstruction (i.e., 3 or 10 d after the release of ureter obstruction) experiments is the demonstration that the peptide- or the endotoxin-induced PGE_2 and TxA_2 release from the perfused kidney was suppressed, whereas the renal cortical and medullary microsomes still exhibited exaggerated cyclooxygenase activity. The high microsomal cyclooxygenase activity present after the release of the ureter obstruction (Table I) might well be attributable to the continued presence of the proliferated activated fibroblasts. Regardless, the elevated capacity to metabolize arachidonate might explain the postobstructive diuresis associated with the release of ureter blockade. A substantial synthesis of urinary prostaglandins might contribute to the reduction in renal vasoconstriction and to the increase in glomerular filtration rate, which occurs at release of ureter obstruction. The cyclooxygenase inhibitor, indomethacin, has been demonstrated to markedly reduce the changes in renal resistance and urine volume in postobstructive diuresis in dogs (31).

In the postobstructed kidneys, there is a paradoxical dissociation between the enzymatic capacity to metabolize arachidonate and the ability of exogenously administered agonists to elicit an arachidonate metabolite release. The morphological studies indicate the continued presence of fibroblasts, but an evident decrease of mononuclear cells (Figs. 5, 6; Table II). The suppressed ability of endotoxin to cause PGE_2 or thromboxane release (Table III) is consistent with the loss of macrophages. The data obtained from the postobstruction experiments further suggest that the presence of the macrophages or of a factor that modulates the fibroblasts is essential for both the basal and the bradykinin-induced arachidonate metabolism. Macrophages are one of the predominant cell types present in chronic inflammatory lesions. Thus, there may be an interesting interplay between the macrophage and fibroblast in renal inflammation.

ACKNOWLEDGMENTS

This work was supported by National Institutes of Health grants HL-14397, HL-20788, and HL-17646, and training grant (to P. Jonas) HL-07275.

REFERENCES

1. Needleman, P., A. H. Kauffman, J. R. Douglas, E. M. Johnson, and G. R. Marshall. 1973. Specific stimulation and inhibition of renal prostaglandin release by angiotensin analogs. *Am. J. Physiol.* **224:** 1415–1419.
2. Larsson, C., and E. Anggard. 1973. Regional differences in the formation and metabolism of prostaglandins in the rabbit kidney. *Eur. J. Pharmacol.* **25:** 326–332.
3. Nishikawa, K., A. R. Morrison, and P. Needleman. 1977. Exaggerated prostaglandin biosynthesis and its influence on renal resistance in the isolated hydronephrotic rabbit kidney. *J. Clin. Invest.* **59:** 1143–1150.
4. Morrison, A. R., K. Nishikawa, and P. Needleman. 1977. Unmasking of thromboxane A_2 synthesis by ureter obstruction in the rabbit kidney. *Nature (Lond.).* **269:** 259–260.
5. Needleman, P., A. Wyche, S. D. Bronson, S. Holmberg, and A. R. Morrison. 1979. Specific regulation of peptide-induced renal prostaglandin synthesis. *J. Biol. Chem.* **254:** 9772–9777.
6. Currie, M. G., B. B. Davis, and P. Needleman. 1981. Localization of exaggerated prostaglandin synthesis associated with renal damage. *Prostaglandins.* **22:** 933–944.
7. Morrison, A. R., K. Nishikawa, and P. Needleman. 1978. Thromboxane A_2 biosynthesis in the ureter obstructed isolated perfused kidney of the rabbit. *J. Pharmacol. Exp. Ther.* **205:** 1–8.
8. Zipser, R., S. Myers, and P. Needleman. 1980. Exaggerated prostaglandin and thromboxane synthesis in the rabbit with renal vein constriction. *Circ. Res.* **47:** 231–237.
9. Benabe, J. E., S. Klahr, M. H. Hoffman, and A. R. Morrison. 1980. Production of thromboxane A_2 by the kidney in glycerol-induced acute renal failure. *Prostaglandins.* **19:** 333–347.
10. Yarger, W. E., D. D. Schocken, and R. H. Harris. 1980. Obstructive nephropathy in the rat. Possible roles for the renin-angiotensin system, prostaglandins, and thromboxanes in postobstructive renal function. *J. Clin. Invest.* **65:** 400–412.
11. Kawasaki, A., and P. Needleman. 1982. Contribution of thromboxane to renal resistance changes in the isolated perfused hydronephrotic rabbit kidney. *Circ. Res.* **50:** 486–490.
12. Nagle, R. B., R. E. Bulger, R. E. Cutter, H. R. Jervis, and E. P. Benditt. 1973. Unilateral obstructive nephropathy in the rabbit. I. Early morphologic, physiologic, and histochemical changes. *Lab. Invest.* **28:** 456–467.
13. Nagle, R. B., M. E. Johnson, and H. R. Jervis. 1976. Proliferation of renal interstitial cells following injury induced by ureteral obstruction. *Lab. Invest.* **35:** 18–22.
14. Eckenfels, A., and J. R. Vane. 1972. Prostaglandins, oxygen tension and smooth muscle tone. *Br. J. Pharmacol.* **45:** 451–462.
15. Smith, W. L., and W. E. M. Lands. 1972. Oxygenation of polyunsaturated fatty acids during prostaglandin biosynthesis by sheep vesicular gland. *Biochemistry.* **11:** 3276–3285.
16. Lysz, T. W., and P. Needleman. 1982. Evidence for two distinct forms of fatty acid cyclooxygenase in brain. *J. Neurochem.* **38:** 1111–1117.
17. Reingold, D. F., K. Waters, S. Holmberg, and P. Needleman. 1981. Differential biosynthesis of prostaglandins by hydronephrotic rabbit and cat kidneys. *J. Pharmacol. Exp. Ther.* **216:** 510–515.
18. Kurland, J. I., and R. Bockman. 1978. Prostaglandin E production by human blood monocytes and mouse peritoneal macrophages. *J. Exp. Med.* **147:** 952–956.
19. Halushka, P. V., J. A. Cook, and W. C. Wise. 1981. Thromboxane A_2 and prostacyclin production by lipopolysaccharide-stimulated peritoneal macrophages. *J. Reticuloendothel. Soc.* **30:** 445–450.
20. Feuerstein, N., M. Foegh, and P. W. Ramwell. 1981. Recently reported stimulation of TxB_2 and 6-keto $PGF_{1\alpha}$ synthesis by rat peritoneal macrophages incubated with *E. coli* 055:BS lipopolysaccharide. *Br. J. Pharmacol.* **72:** 389–391.
21. Schwartzman, M., and A. Raz. 1981. Selective induction of de novo prostaglandin biosynthesis in rabbit kidney cortex. *Biochim. Biophys. Acta.* **664:** 469–474.
22. Martz, E., and M. S. Steinberg. 1972. The role of cell-cell contact in "contact" inhibition of cell-division: a review and new evidence. *J. Cell. Physiol.* **79:** 189–210.
23. Leibovich, S. J., and R. Ross. 1975. The role of the macrophage in wound repair. A study with hydrocortisone and antimacrophage serum. *Am. J. Pathol.* **78:** 71–91.
24. Leibovich, S. J., and R. Ross. 1976. A macrophage-dependent factor that stimulates the proliferation of fibroblasts *in vitro*. *Am. J. Pathol.* **84:** 501–513.
25. Korn, J. H., P. V. Halushka, and E. C. LeRoy. 1980. Mononuclear cell modulation of connective tissue function. Suppression of fibroblast growth by stimulation of endogenous prostaglandin production. *J. Clin. Invest.* **65:** 543–554.
26. D'Souza, S. M., D. J. Englis, A. Clark, and R. G. Russell. 1981. Stimulation of production of prostaglandin E in gingival cells exposed to products of human blood mononuclear cells. *Biochem. J.* **198:** 391–396.
27. Dayer, J-M., D. R. Robinson, S. M. Krane. 1977. Prostaglandin production by rheumatoid synovial cells. Stimulation by a factor from human mononuclear cells. *J. Exp. Med.* **145:** 1399–1404.
28. Humes, J. L., S. Sadowski, M. Galavage, M. Goldenberg, E. Subers, R. J. Bonney, and F. A. Kuehl. 1982. Evidence for two sources of arachidonic acid for oxidative metabolism by mouse peritoneal macrophages. *J. Biol. Chem.* **257:** 1581–1594.
29. Hsueh, W., C. Kuhn, and P. Needleman. 1979. Relationship of prostaglandin secretion by rabbit alveolar macrophages to phagocytosis and lysosomal enzyme release. *Biochem. J.* **184:** 345–354.
30. Dayer, J-M., J. H. Passwell, E. E. Schneeberger, and S. M. Krane. 1980. Interactions among rheumatoid synovial cells and monocyte-macrophages: production of collagenase-stimulating factor by human monocytes exposed to concanavalin A or immunoglobulin Fc fragments. *J. Immunol.* **124:** 1712–1720.
31. Fradet, Y., J. Simmard, J. H. Grose, and M. Lebel. 1980. Enhanced urinary prostagladin E_2 in postobstructive diuresis in humans. *Prostaglandins Med.* **5:** 29–30.